Polymer Bulletin (2023) 80:3633–3647
https://doi.org/10.1007/s00289-022-04220-3

ORIGINAL PAPER

Synthesis and lead ion absorption of magnetic hydrogel nanocomposite absorbents with semi-IPNs structure

Tao Wan[1,2] · Jian Wang[1] · Songsong He[1] · Tairan Wang[1] · Yan Zheng[1] · Fangling Xie[1] · Qi Tang[1]

Received: 5 December 2021 / Revised: 27 February 2022 / Accepted: 27 March 2022 /
Published online: 13 April 2022

Abstract

γ-Methacryloxypropyl trimethoxysilane (KH570)-modified magnetic hydrogel nanocomposite absorbents with semi-interpenetrating networks (semi-IPNs-KH570-mHNAs) were synthesized by radical copolymerization via poly(acrylamide-co-acrylic acid), polyvinyl pyrrolidone (PVP) and KH570-modified magnetic nanoparticles. FTIR and XRD results preliminarily confirmed the target structure of semi-IPNs-KH570-mHNAs without destroying the structure of magnetic nanoparticles during KH570 modification and radical polymerization. Semi-IPNs-KH570-mHNAs with many porous and ravine structure had high adsorption capacity for Pb(II) (450 mg/g). Semi-IPNs-KH570-mHNAs had the best absorption capacity for Pb(II) ion in the synthesis condition of acrylic acid/acrylamide mass ratio of 60:40, 0.8% initiator, acrylic acid (AA) neutralization degree of 70%, 0.2% cross-linker, 12% PVP and 10% KH570-modified magnetic nanoparticles. Besides, semi-IPNs-KH570-mHNAs had good magnetic responsiveness, high thermal stability, reusability which made it a potential application in removing heavy metal ions from the contaminated wastewater.

Introduction

Water pollution by heavy metals is a serious global environmental problem because of their toxic, non-metabolized and non-biodegradable nature. Lead is extensively used in many industrial processes such as electrodeposition and electrophoretic coating [1, 2]. Lead is highly toxic even at very low concentration and

✉ Tao Wan
wantaos@126.com

[1] State Key Lab of Geohazard Prevention and Geoenvironment Protection, Chengdu University of Technology, Chengdu 610059, Sichuan, China

[2] Mineral Resources Chemistry Key Laboratory of Sichuan Higher Education Institutions, Chengdu University of Technology, Chengdu 610059, Sichuan, China

can accumulate in living organisms, interrupting food chain, causing severe disorders and diseases [3]. For example, lead can damage the central nervous system, brain, kidney, liver and reproductive system [4, 5]. Therefore, developing simple and effective methods for Pb(II) removal from water and various industrial wastewater is very important and has attracted a lot of research and practical attention.

To date, numerous methods have been developed for lead removal including reverse osmosis, chemical precipitation, electrodialysis, ultra-filtration and adsorption [6–9]. Among these methods, adsorption has been shown to be a simple, low-cost, efficient, and eco-friendly methodology [10–15]. However, the regeneration and recycling process of conventional adsorbent is complicated [16]. Magnetic nanoadsorbents have been widely paid attention because of their small particle size, large specific surface area, reproducibility and easy solid–liquid separation by using an external magnetic field [17, 18]. However, magnetic nanoadsorbents are easy to oxidize and agglomerate, which decreases their absorption capacity for heavy metals. Hence, in order to avoid its aggregation and increase its stability against oxidation, the surface of magnetic nanoparticles was modified by functional polymers such as natural polymers, e.g., chitosan and its derivatives [18], cellulose [19], poly(1-vinylimidazole) [20] as well as some copolymers, e.g., acrylic acid and crotonic acid [21, 22]. For example, Chen et al. [23] developed a new sulfonated magnetic nanoparticle (Fe_3O_4–SO_3H MNP) by the AMPS branches grafted onto the iron oxide. The Fe_3O_4–SO_3H MNPs showed rapid removal for Pb^{2+} with maximum of adsorption capacity of 108. 93 mg/g at 25 °C. Gautam et al. [24] synthesized biologically magnetic nanoadsorbents from aqueous leaf extract of *Moringa oleifera*to to remove Pb(II) from aqueous solution. The maximum lead adsorption capacities were found to be 49.00, 54.69 and 64.97 mg/g at 30, 40 and 50 °C, respectively.

Hydrogel polymers with three-dimensional networks and functional groups have been widely used in the removal of heavy metals from aqueous solutions because of their abundant functional groups [25–27]. The unique swelling property of hydrogel polymers and the porous structure make heavy metal ions more easily accessible to the three-dimensional networks and be adsorbed by the functional groups in hydrogel polymers. Nanomaterials have been incorporated into the hydrogels in the form of nanocomposite hydrogels in order to improve their mechanical strength [28, 29] or provide a magnetic property [30, 31]. However, few literature has been reported about the synthesis and its lead ion absorption behaviors of γ-methacryloxypropyl trimethoxysilane (KH570)-modified magnetic hydrogel nanocomposite absorbents with semi-IPNs (semi-interpenetrating networks) structure.

In this work, we synthesized KH570-modified magnetic hydrogel nanocomposite absorbents (semi-IPN-KH570-mHNAs) with semi-IPNs structure based on poly(acrylamide-co-acrylic acid), PVP (polyvinyl pyrrolidone) and KH570-modified magnetic nanoparticles. Effect of synthesis parameters such as acrylic acid/acrylamide mass ratio, initiator amount, AA neutralization degree, cross-linker amount and amount of KH570-modified magnetic nanoparticles on the Pb(II) adsorption capacities were investigated. Structure, morphologies and reusability of semi-IPNs-KH570-mHNAs were also evaluated.

Materials and methods

Materials

Acrylic acid (AA), acrylamide (AM), ammonium persulfate (APS), and sodium bisulfite (SBS) were purchased from Chengdu Kelong Reagent Chemicals (China). Ferric trichloride hexahydrate ($FeCl_3 \cdot 6H_2O$), ferrous chloride heptahydrate ($FeCl_2 \cdot 7H_2O$) and γ-methacryloxypropyl trimethoxysilane (KH570) were purchased from Chengdu Huaxia Reagent Chemicals (China). Polyvinyl pyrrolidone (PVP) and *N*,*N*-methylene bisacrylamide (MBA) were purchased from Chengdu Aike Chemical Reagent (China). All chemicals used were of analytical reagent grade without further purification.

Preparation of magnetic nanoparticles (MNPs)

Magnetic nanoparticles (MNPs) were synthesized according to the reported procedure by co-precipitation method [32–34]. Typically, 19.6 g $FeCl_3 \cdot 6H_2O$ and 7.2 g $FeCl_2 \cdot 7H_2O$ were dissolved in deionized water (300 mL) and stirred at 60 °C. Then, 2 mol/L of ammonia solution was added dropwise under vigorous stir until the pH reached 11 and the reaction mixture was stirred for 4.5 h. After cooling down to room temperature, the magnetic nanoparticles were separated by an external magnet and washed several times with deionized water. Finally, the magnetic nanoparticles were dried at 60 °C for 24 h under vacuum.

Preparation of KH570-modified magnetic nanoparticles (KH570-MNPs)

Typically, 1 g magnetic nanoparticles were dissolved in deionized water and ethanol (100 mL) with water/ethanol volume ratio of 1:1 and stirred at 50 °C under N_2 protection. Then, 1.5 mL 30% ammonia solution was added dropwise under vigorous stir, followed by slow addition of 3 mL silane coupling agent (KH570) under vigorous stirring. After 4 h reaction under N_2 protection, the temperature was cooled down to room temperature and KH570-modified magnetic nanoparticles were separated by an external magnet and washed several times with deionized water and ethanol alternately. Finally, KH570-modified magnetic nanoparticles were dried at 60 °C for 24 h under vacuum.

Preparation of KH570-modified magnetic hydrogel nanocomposites absorbents (semi-IPNs-KH570-mHNAs)

Typically, the synthesis of KH570-modified magnetic hydrogel nanocomposite absorbents (semi-IPNs-KH570-mHNAs) is as follows: 10 g acrylic acid, 10 g acrylamide,2.4 g PVP and 3.61 g NaOH were dissolved in 100 mL deionized water and stirred for 45 min at room temperature. Then, 2 g KH570-modified magnetic nanoparticles and 0.04 g MBA were added into the above monomer solution and stirred for 30 min at room temperature. After that, the temperature was raised to

60℃, followed by the slow addition of 0.24 g ammonium persulfate and 0.077 g sodium bisulfite. The reaction mixture was stirred for 5 h at 60 ℃. After cooling down to room temperature, semi-IPNs-KH570-mHNAs were separated by an external magnet, washed several times with deionized water and ethanol alternately and left over night in ethanol. Finally, semi-IPN-KH570-mHNAs were dried at 60 °C for 24 h under vacuum. Scheme for the synthesis route of semi-IPN-KH570-mHNAs is shown in Fig. 1.

Lead ion adsorption experiment using batch methods

Batch adsorption experiments were carried out on a thermostatic shaker with a constant speed of 120 rpm at room temperature to study adsorption properties of lead ion for semi-IPNs-KH570-mHNAs. 0.1 g dry and milled semi-IPNs-KH570-mHNAs was immersed in 100 mL lead ion solution with desired initial concentration (1200 mg/L) and pH (4.5) for a given time (120 min) at room temperature, and then lead ion concentration left in the solution was analyzed by atomic absorption spectrometry.

Metal absorption capacity is calculated using the following equation:

$$q_e = \left(C_0 - C_e\right)V/m \tag{1}$$

where q_e is the amount of metal ion adsorbed (mg/g), C_0 and C_e are initial and equilibrium concentration of metal ion (mg/L) in the testing solution, respectively. V is the volume of the metal ion solution (L) and m is the mass of dry semi-IPNs-KH570-mHNAs (g).

Desorption and regeneration experiments for semi-IPNs-KH570-mHNAs toward lead ion

Desorption of lead ion is carried out in 0.5 M HCl solution (50 mL) for 90 min. After a given time, the supernatant was subjected to determine the concentration of lead ion by atomic absorption spectrometry and desorption percentage is calculated according to Eq. (2).

$$\text{Desorption} = M_d/M_0 \times 100\% \tag{2}$$

where M_0 is the amount of heavy metal ions adsorbed by semi-IPNs-KH570-mHNAs and M_d is the amount of lead ion desorbed.

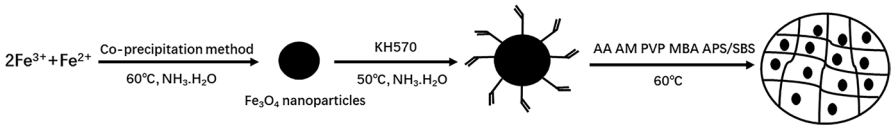

Fig. 1 Scheme for the synthesis route of semi-IPN-KH570-mHNAs

After desorption, semi-IPNs-KH570-mHNAs were removed from desorption solution using an external magnet, and washed with distilled water, dried at 60 °C for 24 h, and used for the subsequent runs. To test the reusability of semi-IPNs-KH570-mHNAs, this adsorption–desorption cycle was repeated five times using the same adsorbents.

Characterization of the magnetic hydrogel nanocomposite absorbents

Morphologies of magnetic nanoparticles and KH570-modified magnetic nanoparticles were observed by JEM-100CX transmission electron microscopy (TEM). The samples were dropped onto a lead net sprayed with carbon, dried in vacuum, and then tested on a transmission electron microscope with an acceleration voltage of 100 kV. Micrographs of semi-IPNs-KH570-mHNAs were observed by HITACHI S-530 scanning electron microscope (SEM). Before SEM observation, all samples were fixed on aluminum stubs and coated with gold. FTIR spectrum was carried out on a Perkin–Elmer 1750 spectrophotometer, equipped with an Epson Endeavour II data station. The samples were prepared as KBr pellets or as liquid films interposed between KBr disks. X-ray diffraction analysis was carried out on DMX-IIIC diffractometer. Magnetic properties were determined by a LakeShore 7407 vibrating sample magnetometer (VSM) at room temperature. Thermogravimetric analysis (TGA) was carried out from room temperature to 600 ℃ with a heating rate of 10 ℃/min under steady nitrogen.

Results and discussion

TEM and SEM characterization of the magnetic materials

Figure 2a, b shows the TEM images of magnetic nanoparticles, and KH570-modified magnetic nanoparticles, respectively. The magnetic nanoparticles and silane coupling agent-modified magnetic nanoparticles have average size of 15–30 nm with irregular particle shape and partial agglomeration. This may be ascribed to the fact that magnetic nanoparticles are easy to agglomerate during high vacuum drying process of TEM. After surface modification with silane coupling agent (KH570), agglomeration of magnetic nanoparticles is reduced due to the steric effect and repulsion of organic molecules grafted onto magnetic nanoparticles. Besides, the above TEM results demonstrate that unmodified and KH570-modified magnetic particles with nanometer size are successfully synthesized by coprecipitation method. As indicated in Fig. 2c, semi-IPNs-KH570-mHNAs has rough and uneven surface with many porous and ravine structure. The structure with high specific surface area can make heavy metal ions easily and rapidly penetrate into the three-dimensional network of magnetic polymer adsorbents, thus upgrading the heavy metal adsorption for magnetic polymer adsorbent.

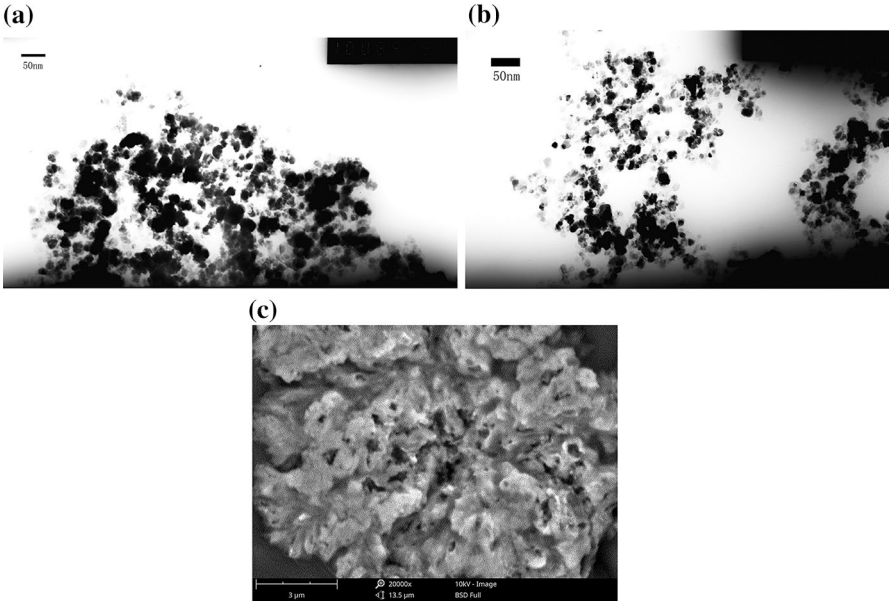

Fig. 2 TEM images of magnetic nanoparticles (**a**), KH570-MNPs (**b**). SEM image of semi-IPNs-KH570-mHNAs (**c**)

FTIR and XRD analysis of the magnetic materials

Figure 3a demonstrates XRD patterns of magnetic Fe_3O_4 nanoparticles, KH570-modified magnetic nanoparticles and semi-IPNs-KH570-mHNAs. Both magnetic Fe_3O_4 nanoparticles, KH570-modified magnetic nanoparticles and semi-IPNs-KH570-mHNAs, have characteristic diffraction peaks for the standard pattern of Fe_3O_4 (JCPDS No. 85-1436) which appear at $2\theta = 30.53°$, 35.59°, 43.36°, 53.96°, 57.45° and 62.92°, respectively. These diffraction peaks are ascribed to (220), (311), (400), (422), (511) and (440) in the cubic phase of pure Fe_3O_4, respectively. In

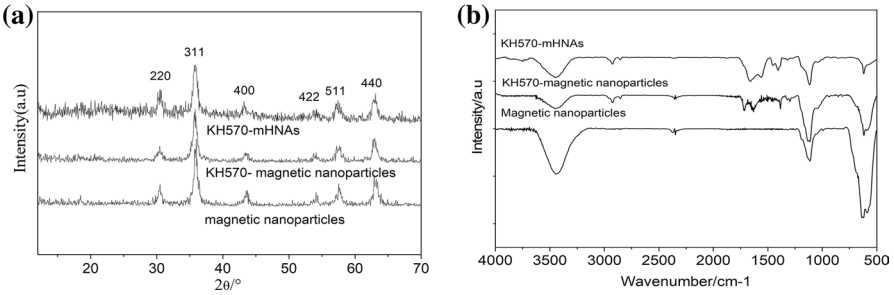

Fig. 3 FTIR spectra (**a**) and XRD spectra (**b**) of magnetic nanoparticles, KH570-MNPs and semi-IPNs-KH570-mHNAs

addition, it is found that the position of the diffraction peaks for three samples is basically unchanged with no impurity peaks. This shows that the crystal structure of Fe_3O_4 does not change during KH570 modification and radical polymerization.

Figure 3b shows FTIR spectra of magnetic Fe_3O_4 nanoparticles, KH570-modified magnetic nanoparticles and semi-IPNs-KH570-mHNAs. As seen in the spectrum of unmodified magnetic nanoparticles, 3445 cm^{-1} and 1113 cm^{-1} are attributed to the O–H stretching and bending vibration. The sharp peaks near 619 cm^{-1} are attributed to the Fe–O functional group [35, 36]. This indicates that Fe_3O_4 nanoparticles prepared by the co-precipitation method have active hydroxyl groups on the surface, which creates the possibility for post-surface modification. As seen from FTIR spectrum of KH570-modified magnetic nanoparticles, the absorption peaks at 2920 cm^{-1} and 2850 cm^{-1} are $–CH_2–$ stretching vibration, 1715 cm^{-1} is attributed to C=O stretching vibration, 1640 cm^{-1} is assigned to the stretching vibration of C=C, 1388 cm^{-1} is ascribed to the stretching vibration of C=O, and 1130 cm^{-1} is the stretching vibration peak of Si–O [37], which indicates that the KH570 has been successfully grafted onto the surface of magnetic Fe_3O_4 nanoparticles. After radical copolymerization, the spectrum changes obviously. 3760 cm^{-1} and 1564 cm^{-1} are the stretching and bending vibration of NH group, 1405 cm^{-1} is the C–N stretching vibration [37], 1609 cm^{-1} and 1418 cm^{-1} are anti-symmetrical vibration and symmetrical vibration absorption of $–COO^-$, and 1715 cm^{-1} is the carbonyl absorption. From the above FTIR spectra, it can be inferred that the KH570-modified magnetic nanoparticles have copolymerized with acrylic acid, acrylamide in the presence of PVP and semi-IPNs-KH570-mHNAs with target structure has been successfully synthesized.

Magnetic property and TGA analysis of the magnetic materials

The hysteresis curves of magnetic Fe_3O_4 nanoparticles, KH570-modified magnetic nanoparticles and semi-IPNs-KH570-mHNAs are shown in Fig. 4a. It can be seen that the saturation magnetization of magnetic Fe_3O_4 nanoparticles, KH570-modified magnetic nanoparticles and magnetic polymer absorbents are 67.7 emu/g, 57.3 emu/g and 20.4 emu/g, respectively. After KH570 modification

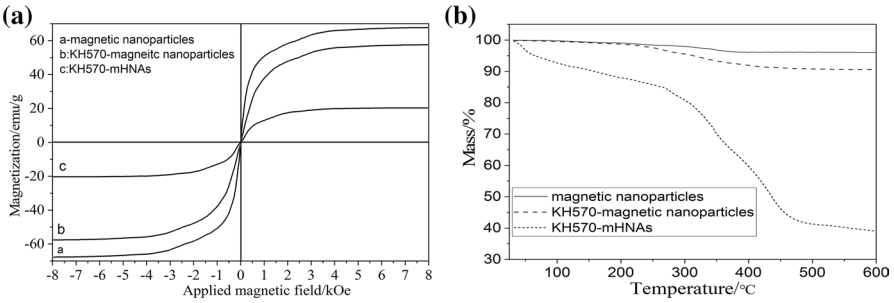

Fig. 4 Magnetization curves (**a**) and TGA (**b**) of magnetic nanoparticles, KH570-MNPs and semi-IPNs-KH570-mHNAs

and copolymerization, saturation magnetization decreases due to the non-magnetic response for silane coupling agent KH570 and the polymer matrix. However, semi-IPNs-KH570-mHNAs still have a certain magnetic response. Besides, the remanence and coercivity of the three samples tend to be zero, showing superparamagnetic behavior. Hence, the magnetic solid–liquid separation characteristics of the magnetic polymer adsorbents make it have broad application prospects in the field of heavy metal ions removal.

As indicated in Fig. 4b, TGA curve of magnetic Fe_3O_4 nanoparticles showed slight weight loss (3.8%) around 600 °C, which should be resulted from the dehydration of hydroxyl groups on the surface of magnetic Fe_3O_4 nanoparticles. Weight loss of KH570-modified magnetic nanoparticles reaches 6.5% from 200 to 600 ℃ due to the decomposition of the silane coupling agent grafted onto the surface of magnetic nanoparticles, indicating that silane coupling agent is successfully grafted onto the surface of magnetic nanoparticles with the content of about 6.5%. The weight loss for semi-IPNs-KH570-mHNAs between 30 and 200 ℃ can be attributed to a small amount of evaporation of adsorbed water. Weight loss of semi-IPNs-KH570-mHNAs reaches 38% between 290 and 500 ℃ which is mainly ascribed to decomposition of polymeric matrix chains, as well as silane coupling agent grafted onto magnetic nanoparticles. It is worth noting that the onset thermal decomposition temperature of semi-IPNs-KH570-mHNAs exceeds 292 ℃, indicating high thermal stability of semi-IPNs-KH570-mHNAs.

Effect of AA/AM mass ratio on lead ion adsorption capacity of semi-IPNs-KH570-mHNAs

The influence of AA/AM mass ratio on lead ion adsorption capacity of semi-IPNs-KH570-mHNAs is shown in Fig. 5.With the increase in AA/AM mass ratio, lead ion adsorption capacity of semi-IPNs-KH570-mHNAs increased firstly, reaching the maximum in the condition of AA/AM mass ratio of 60:40, and then decreased with increased AA/AM mass ratio. Generally, both carboxyl and amide groups can absorb heavy metal ions. COO^- can absorb heavy metal ions through complexation and electrostatic interaction with heavy metal ions, while CONH2 absorbs heavy

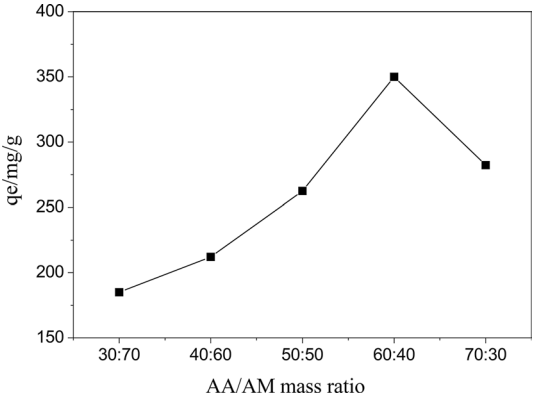

Fig. 5 Effects of AA/AM mass ratio on the adsorption capacity of lead ion for semi-IPNs-KH570-mHNAs

metal ions through complexation. Therefore, COO^- groups have higher absorption capacity for heavy metal ions than $CONH_2$ groups, and a higher AA/AM mass ratio can improve the adsorption capacity of magnetic polymer adsorbents for heavy metals. However, too high AA/AM mass ratio will reduce the adsorption of heavy metals for semi-IPNs-KH570-mHNAs. The higher the concentration of acrylic acid, the greater the reactivity of the monomer and the faster the speed of radical copolymerization, resulting in a rapid increase in temperature during free radical copolymerization. This will decrease molecular weight between the network mesh, reducing the mesh size and forming a dense polymer network structure, which makes it difficult for heavy metal ions penetrate into the polymer gel network, and reduces the absorption capacity of heavy metal ions for semi-IPNs-KH570-mHNAs.

Effect of AA neutralization degree on lead ion adsorption capacity of semi-IPNs-KH570-mHNAs

Figure 6 shows the effects of neutralization degree of AA on lead ion adsorption capacity of semi-IPNs-KH570-mHNAs. Pb(II) adsorption capacity of semi-IPNs-KH570-mHNAs increases first and then decreases with the increase in AA neutralization degree. When AA neutralization degree is 70%, Pb(II) adsorption capacity of semi-IPNs-KH570-mHNAs reaches the maximum.

When acrylic acid is neutralized, a stable p-π conjugated structure will form due to the electron donor characteristic of carboxyl anion, thereby reducing the free radical reactivity of acrylic acid. Therefore, the greater the neutralization degree of acrylic acid, the lower the reactivity of acrylic acid. When the neutralization degree of acrylic acid is low, copolymerization reactivity is relatively high due to the high reactivity of AA under acidic condition, causing rapid copolymerization reaction rate, sharp temperature rise, and the formation of dense polymer networks. In addition, under acidic conditions, COOH on the polymer molecular chains is difficult to ionize, resulting in a small electrostatic repulsion between polymer molecular chains, which makes it difficult for lead ion to penetrate into the 3D polymer network, and thus reduces lead ion adsorption capacity for semi-IPNs-KH570-mHNAs.

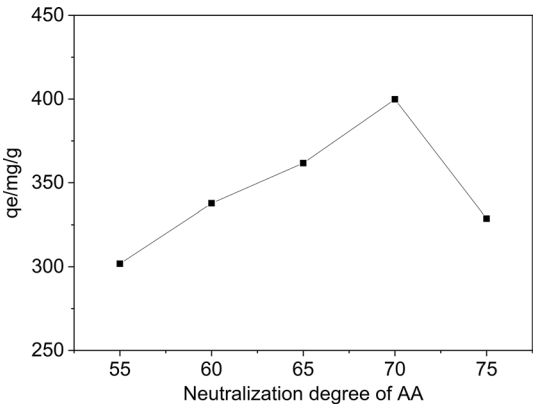

Fig. 6 Effects of neutralization degree of AA on the adsorption capacity of lead ion for semi-IPNs-KH570-mHNAs

When AA neutralization degree is greater than 70%, more counterion Na^+ will exist within the polymer network, leading to an increased shielding effect and reduction in the electrostatic repulsive force between the polymeric chains, which is not beneficial to the expansion of the polymer three-dimensional network, and decreases the adsorption capacity of lead ion for semi-IPNs-KH570-mHNAs.

Effect of cross-linker amount on lead ion adsorption capacity of semi-IPNs-KH570-mHNAs

Cross-linker plays an important role on the cross-linking density, rigidity and strength of the polymer networks, and thus finally affects the heavy metals adsorption of the adsorbents. Figure 7 shows the influence of the amount of cross-linker (based on AA and AM mass) on lead ion adsorption capacity of semi-IPNs-KH570-mHNAs. When the amount of cross-linker is less than 0.2%, lead adsorption capacity of semi-IPNs-KH570-mHNAs increases with the increase in the amount of cross-linker. When the amount of cross-linker is greater than 0.2%, lead adsorption capacity of semi-IPNs-KH570-mHNAs decreases gradually.

It is difficult to form a slightly cross-linked polymeric network when the amount of cross-linker is low, which is not in favor of the adsorption of lead ion. However, excessive cross-linker will further increase the cross-linking density of the polymer network, forming more densely and rigidly polymer three-dimensional networks, making it difficult for lead ion to penetrate into polymer networks. Therefore, semi-IPNs-KH570-mHNAs prepared with appropriate amount of cross-linker has good adsorption capacity of lead ion.

Effect of initiator amount on lead ion adsorption capacity of semi-IPNs-KH570-mHNAs

Figure 8 shows the influence of the amount of initiator (based on AA and AM mass) on lead ion adsorption capacity of semi-IPNs-KH570-mHNAs. As can

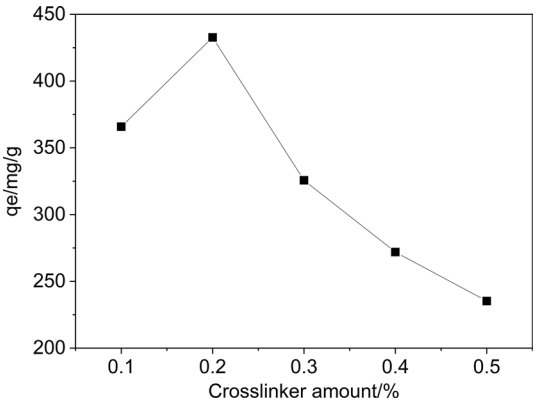

Fig. 7 Effects of cross-linker amount on the adsorption capacity of lead ion for semi-IPNs-KH570-mHNAs

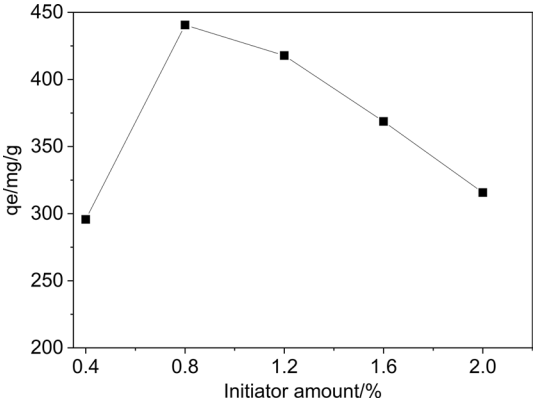

Fig. 8 Effects of initiator amount on the adsorption capacity of lead ion for semi-IPNs-KH570-mHNAs

be seen from Fig. 7, lead ion adsorption capacity of semi-IPNs-KH570-mHNAs reaches the maximum when initiator amount is 0.8%. Initiator amount higher or lower than 0.8% will both reduce lead ion adsorption capacity for semi-IPNs-KH570-mHNAs. When initiator amount is less than 0.8%, the reaction system has few free radicals, which leads to a low reaction rate and is not beneficial to the formation of three-dimensional network structure. On the other hand, excess initiator can decompose and release a number of free radicals which can reduce the molecular weight between meshes of the networks, making polymer network more dense and heavy metal ions more difficult to diffuse into the polymeric network. Hence, too low or too high amount of initiator will both reduce lead ion adsorption capacity for semi-IPNs-KH570-mHNAs.

Effect of amount of KH570-modified magnetic nanoparticles on lead ion adsorption capacity of semi-IPNs-KH570-mHNAs

Figure 9 demonstrates the influence of the amount of KH570-modified magnetic nanoparticles (based on AA and AM mass) on lead ion adsorption capacity of semi-IPNs-KH570-mHNAs. Lead ion absorption capacity increased when the amount of KH570-modified magnetic nanoparticles increased from 5 to 10% and then decreased with further increasing amount of KH570-modified magnetic nanoparticles. KH570-modified magnetic nanoparticles have polymerizable double bonds on the surface and can copolymerize with functional monomers to form a three-dimensional network structure. Therefore, the increase in the amount of KH570-modified magnetic nanoparticles can help the formation of three-dimensional network structure and increase lead ion adsorption capacity of the magnetic polymer adsorbents. However, too much KH570-modified magnetic nanoparticles will further increase the cross-linking density and rigidity of the polymer network, which is not conducive to the diffusion and penetration of heavy metal ions into the polymer network, thus decreasing lead ion adsorption capacity of semi-IPNs-KH570-mHNAs.

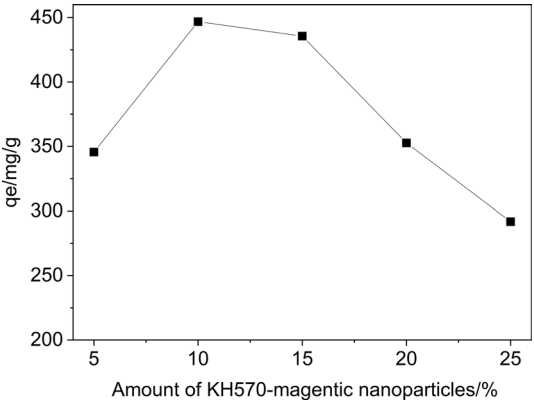

Fig. 9 Effects of amount of KH570-modified magnetic nanoparticles on adsorption capacity of lead ion for semi-IPNs-KH570-mHNAs

Effect of PVP amount on lead ion adsorption capacity of semi-IPNs-KH570-mHNAs

Figure 10 shows the effect of PVP amount (based on AA and AM mass) on lead ion adsorption capacity of semi-IPNs-KH570-mHNAs. Lead ion adsorption capacity of semi-IPNs-KH570-mHNAs increases first and then decreases with the increase in PVP amount. When PVP amount is 12%, lead ion adsorption capacity of semi-IPNs-KH570-mHNAs reaches the maximum (450 mg/g). Polyvinylpyrrolidone (PVP) has a pyrrolidone group with good heavy metal ion adsorption. During free radical copolymerization, a semi-interpenetrating network structure (semi-IPNs) is formed, in which PVP is dispersed in the three-dimensional polymer network structure. This can improve the elasticity and extensibility of the polymeric network and increase lead ion adsorption capacity of semi-IPNs-KH570-mHNAs. On the other hand, when PVP amount exceeds 12%, excess PVP will further increase the chain entanglement between the macromolecular chains and increase the physical cross-link density of the polymer network, which is not conducive to the diffusion of heavy metal ions into the polymeric network. Therefore, lead ion adsorption capacity of magnetic polymer adsorbents is reduced.

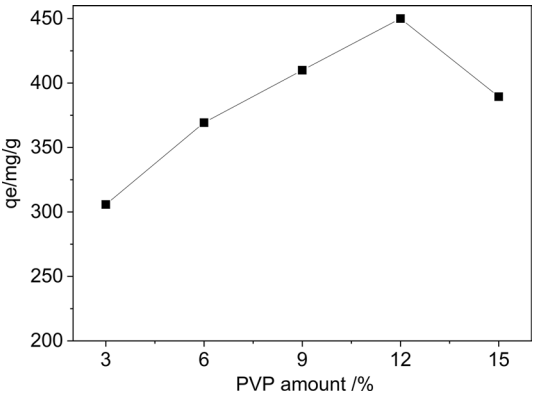

Fig. 10 Effects of PVP amount on adsorption capacity of lead ion for semi-IPNs-KH570-mHNAs

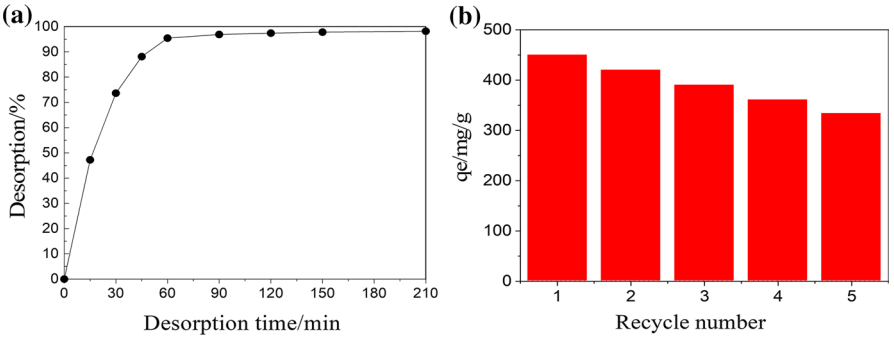

Fig. 11 Desorption-regeneration performance for semi-IPNs-KH570-mHNAs toward lead ion

Desorption-regeneration performance of semi-IPNs-KH570-mHNAs toward lead ion

It is well known that the recyclability and stability of the adsorbent are crucial for practical applications of the adsorbent. Therefore, continuous adsorption–desorption experiments were performed to evaluate the reusability of semi-IPNs-KH570-mHNAs. Figure 11a shows the desorption curves of semi-IPNs-KH570-mHNAs using hydrochloric acid as desorbent. Desorption of Pb(II) by hydrochloric acid reached equilibrium after 60 min with desorption efficiency of 95%, indicating that aqueous HCl can successfully desorb Pb(II) from semi-IPNs-KH570-mHNAs. After five cycles, semi-IPNs-KH570-mHNAs has Pb(II) absorption capacity of 333.5 mg/g which reached 74% of that (450 mg/g) for the first absorption, as indicated in Fig. 11b. This indicates good reversibility and recyclability of semi-IPNs-KH570-mHNAs. The decrease in absorption capacity may be caused by a few active sites not being released or incomplete desorption.

Conclusion

KH570-modified magnetic hydrogel nanocomposites with semi-IPNs structure (semi-IPNs-KH570-mHNAs) were prepared by radical copolymerization of acrylamide and acrylic acid in the presence of KH570-modified magnetic nanoparticles and PVP. FTIR and XRD results show that semi-IPNs-KH570-mHNAs have been successfully prepared without destroying high crystallinity of magnetic Fe_3O_4. Semi-IPNs-KH570-mHNAs have high adsorption capacity of Pb(II) (450 mg/g) due to its porous and ravine structure and multiple adsorption groups. Semi-IPNs-KH570-mHNAs had the maxima absorption capacity for Pb(II) ion in the synthesis condition of AA/AM mass ratio of 60:40, 0.8% initiator, AA neutralization degree of 70%, 0.2% cross-linker, 12% PVP and 10% KH570-modified magnetic nanoparticles. In addition, semi-IPNs-KH570-mHNAs had good magnetic responsiveness, thermal stability and recycling performance, making it potential applications in removing heavy metal ions from the aqueous solution.

Acknowledgements This work was supported by the Key Research and Development Program of Sichuan province (Grant No. 2019YFG0264); Technology Foundation for Selected Overseas Chinese Scholar, Department of Personnel of Sichuan province (Grant No. 19BZ08-009); State Key Laboratory of Geohazard Prevention and Geoenvironment Protection (Grant No. SKLGP2018Z005).

References

1. Ruparelia J, Duttagupta S, Chatterjee A, Mukherji S (2008) Potential of carbon nanomaterials for removal of heavy metals from water. Desalination 232(1):145–156
2. Mubarak N, Alicia R, Abdullah E, Sahu J, Haslija AA, Tan J (2013) Statistical optimization and kinetic studies on removal of Zn^{2+} using functionalized carbon nanotubes and magnetic biochar. J Environ Chem Eng 1(3):486–495
3. Acharya S, Dilnawaz F, Sahoo SK (2009) Targeted epidermal growth factor receptor nanoparticle bioconjugates for breast cancer therapy. Biomaterials 30(29):5737–5750
4. Gurer-Orhan H, Sabir HU, Ozgunes H (2004) Correlation between clinical indicators of lead poisoning and oxidative stress parameters in controls and lead-exposed workers. Toxicology 195:147–154
5. Moradi A, Moghadam PN, Hasanzadehb R, Sillanpaa M (2017) Chelating magnetic nanocomposite for the rapid removal of Pb(II) ions from aqueous solutions: characterization, kinetic, isotherm and thermodynamic studies. RSC Adv 7:433
6. Mishra A, Nath A, Pande PP, Shankar R (2021) Treatment of gray wastewater and heavy metal removal from aqueous medium using hydrogels based on novel crosslinkers. J Appl Polym Sci 138:50242
7. Joshiba GJ, Kumar PS, Christopher FC, Pooja G, Kumar VV (2020) Fabrication of novel amine-functionalized magnetic silica nanoparticles for toxic metals: kinetic and isotherm modeling. Environ Sci Pollut Res 27:27202–27210
8. Saravannan A, Kumar PS, Renita AA (2018) Hybrid synthesis of novel material through acid modification followed ultrasonication to improve adsorption capacity for zinc removal. J Clean Prod 172:92–105
9. Semerjian L (2018) Removal of heavy metals (Cu, Pb) from aqueous solutions using pine (*Pinus halepensis*) sawdust: equilibrium, kinetic, and thermodynamic studies. Environ Technol Innov 12:91–103
10. Cegłowskia M, Gierczyka B, Frankowskia M, Popendab L (2018) A new low-cost polymeric adsorbents with polyamine chelating groups for efficient removal of heavy metal ions from water solutions. React Funct Polym 131:64–74
11. Hemavathy RRV, Kumar PS, Suganya S, Swetha V, Varjani SJ (2019) Modelling on the removal of toxic metal ions from aquatic system by different surface modified *Cassia fistula* seeds. Bioresour Technol 281:1–9
12. Afkhami A, Norooz-Asl R (2009) Removal, preconcentration and determination of Mo(VI) from water and wastewater samples using maghemite nanoparticles. Colloids Surf A Physicochem Eng Asp 346:52–57
13. Chen F, Wu Q, Lü Q, Xu Y, Yu Y (2015) Synthesis and characterization of bifunctional mesoporous silica adsorbent for simultaneous removal of lead and nitrate ions. Sep Purif Technol 151:225–231
14. Luzardo FHM, Velasco FG, Correia IKS, Silva PMS, Salay LC (2017) Removal of lead ions from water using a resin of mimosa tannin and carbon nanotubes. Environ Technol Innov 7:219–228
15. Yin N, Wang K, Ya X, Li Z (2018) Novel melamine modified metal organic frameworks for remarkably high removal of heavy metal Pb(II). Desalination 430:120–127
16. Neeraj G, Krishnan S, Kumar PS, Shriaishvarya KV, Kumar VV (2015) Performance study on sequestration of lead ions from contaminated water using newly synthesized high effective chitosan coated magnetic nanoparticles. J Mol Liq 214:335–346
17. Tang SCN, Lo IMC (2013) Magnetic nanoparticles: essential factors for sustainable environmental applications. Water Res 47:2613–2632
18. Liu X, Hu Q, Fang Z, Zhang X, Zhang B (2009) Magnetic chitosan nanocomposites: a useful recyclable tool for heavy metal ion removal. Langmuir 25:3–8
19. Xiong R, Wang YR, Zhang XX, Lu CH (2014) Facile synthesis of magnetic nanocomposites of cellulose@ultrasmall iron oxide nanoparticles for water treatment. RSC Adv 4:22632

20. Shan C, Ma Z, Tong M, Ni J (2015) Removal of Hg(II) by poly(1-vinylimidazole)-grafted Fe_3O_4@SiO2 magnetic nanoparticles. Water Res 69:252–260
21. Ge F, Li MM, Ye H, Zhao BX (2012) Effective removal of heavy metal ions Cd^{2+}, Zn^{2+}, Pb^{2+}, Cu^{2+} from aqueous solution by polymer-modified magnetic nanoparticles. J Hazard Mater 211–212:366–372
22. Jiang LP, Liu P (2014) Design of magnetic attapulgite/fly ash/poly(acrylic acid) ternary nanocomposite hydrogels and performance evaluation as selective adsorbent for Pb^{2+} ion. ACS Sustain Chem Eng 2:1785–1794
23. Chen K, He J, Li Y, Cai X, Zhang K, Liu T, Hu Y, Lin D, Kong L, Liu J (2017) Removal of cadmium and lead ions from water by sulfonated magnetic nanoparticle adsorbents. J Colliod Interf Sci 494:307–316
24. Gautam PK, Shivalkar S, Banerjee S (2020) Synthesis of *M. oleifera* leaf extract capped magnetic nanoparticles for effective lead [Pb (II)] removal from solution: Kinetics, isotherm and reusability study. J Mol Liq 305:112811
25. Wan H, Han YJ, Liu Y, Bai T, Gao H, Zhang P, Wang W, Liu WG (2012) High-strength hydrogel as a reusable adsorbent of lead ions. J Hazard Mater 213:258–264
26. Ramirez E, Burillo SG, Barrera-Diaz C, Roa G, Bilyeu B (2011) Use of pH-sensitive polymer hydrogels in lead removal from aqueous solution. J Hazard Mater 192:432–439
27. Milosavljevic NB, Ristic MD, Peric-Grujic AA, Fillipovic JM, Strbac SB, Rakocevic ZL, Krusic MTK (2011) Sorption of zinc by novel pH-sensitive hydrogels based on chitosan, itaconic acid and methacrylic acid. J Hazard Mater 192:846–854
28. Saber-Samandari S, Saber-Samandari S, Gazi M (2013) Cellulosegraft-polyacrylamide/hydroxyapatite composite hydrogel with possible application in removal of Cu(II) ions. React Funct Polym 73:1523–1530
29. Natkanski P, Kustrowski P, Bialas A, Piwowarska Z, Michalik M (2013) Thermal stability of montmorillonite polyacrylamide and polyacrylate nanocomposites and adsorption of Fe(III) ions. Appl Clay Sci 75–76:153–157
30. Yu ZH, Zhang XD, Huang YM (2013) Magnetic chitosaniron(III) hydrogel as a fast and reusable adsorbent for chromium(VI) removal. Ind Eng Chem Res 52:11956–11966
31. Yan H, Yang LY, Yang Z, Yang H, Li AM, Cheng RS (2012) Preparation of chitosan/poly(acrylic acid) magnetic composite microspheres and applications in the removal of lead(II) ions from aqueous solutions. J Hazard Mater 229:371–380
32. Kumar PS, Senthamarai C, Durgadevi A (2014) Adsorption kinetics, mechanism, isotherm, and thermodynamic analysis of lead ions onto the surface modified agricultural waste. Environ Prog Sustain Energy 33:28–37
33. Kumar VV, Sivanesan S, Cabana H (2014) Magnetic cross-linked laccase aggregates—bioremediation tool for decolorization of distinct classes of recalcitrant dyes. Sci Total Environ 487:830–839
34. Paripoorani KS, Ashwin G, Vengatpriya P, Ranjitha V, Rupasree S, Kumar VV (2015) Insolubilisation of inulinase on magnetite chitosan micro-particles, an easily recoverable and reusable support. J Mol Catal B Enzym 113:47–55
35. Chandra S, Bhattacharya J (2019) Influence of temperature and duration of pyrolysis on the property heterogeneity of rice straw biochar and optimization of pyrolysis conditions for its application in soils. J Clean Prod 215:1123–1139
36. Sun Y, Yu IKM, Tsang DCW, Cao X, Lin D, Wang L, Graham NJD, Alessi DS, Komárek M, Sik Y, Feng Y (2019) Multifunctional iron-biochar composites for the removal of potentially toxic elements, inherent cations, and hetero-chloride from hydraulic fracturing wastewater. Environ Int 124:521–532
37. Shi S, Yang J, Liang S, Li M, Gan Q, Xiao K, Hu J (2018) Enhanced Cr(VI) removal from acidic solutions using biochar modified by Fe_3O_4@SiO_2–NH_2 particles. Sci Total Environ 628–629:499–508